

Frictional effects on the cyclic response of laterally loaded timber fasteners

Nii Allotey†

Department of Civil and Environmental Engineering, The University of Western Ontario, Canada

Ricardo Foschi‡

Department of Civil Engineering, The University of British Columbia, Canada

(Received September 9, 2004, Accepted June 2, 2005)

Abstract. Foschi's connector model is used as a basic component in the development of nonlinear analysis programs for timber structures. This paper presents the extension of the model to include the effect of shaft frictional forces. The wood medium is modeled using the Foschi embedment model, while shaft friction is modeled using an elastic Coulomb-type friction model. The initial confining pressure for the case of driven fasteners is accounted for by a lateral shift of the load-embedment curve. The model is used to compute the cyclic response of both driven and inserted fasteners. The results obtained from the cases studied indicate that initial confining pressure and friction do not have a significant effect on the computed hysteretic response, however, they significantly affect the computed amount of fastener withdrawal. This model is particularly well-suited for modeling the hysteretic response of shear walls with moderate fastener withdrawal under lateral cyclic or earthquake loading.

Key words: mechanics-based model; timber fastener; cyclic; load-embedment curve; finite element; withdrawal; friction; initial confining pressure; earthquake.

1. Introduction

Due to a number of major failures from hurricanes and earthquakes, the need for improved design methods for various structures has been generally noted. To ensure the proper design of such structures, there is a need to understand the characteristics of the response of each structural component, and also the global response of the whole structure.

Due to the brittle failure characteristic of wood in tension, the overall response of timber structures is governed directly by the response of the fasteners. More complex deformation mechanisms occur under cyclic or dynamic loading than for monotonic loading. Some of the factors that account for this behavior are, growth of fastener hole size due to local crushing of wood fiber and the degradation of stiffness and strength due to cycling action.

Different approaches have been developed to model the response of the connector. These can be

† Research Assistant, Corresponding author, E-mail: nkallote@uwo.ca

‡ Professor

grouped into: single degree-of-freedom (SDOF) lumped parameter models, which have a set of rules for unloading and reloading (Foliente 1995, Folz and Filialtraut 2001); mechanics-based approaches, which involve modeling the wood-fastener system as a beam-on-a-linear or nonlinear Winkler foundation (Foschi 2000, Chui *et al.* 1998), and numerical approaches, that are based on the full modeling of the wood medium with finite elements (e.g., Moses 2000, Guan and Rodd 2000). The single degree-of-freedom (SDOF) lumped parameter models often involve a number of parameters that have to be calibrated from experiments for different types of connections. Also, although the numerical approach is very sophisticated, it is computationally expensive when used in modeling entire shear wall or frame building systems.

The mechanics-based approach, also called the “component approach” uses basic material properties such as the wood embedment response and fastener stress-strain response as input variables. The model by Chui *et al.* (1998) was developed within the context of a total lagrangian formulation and is based on using a set of loading/reloading rules that are characterized by parameters defined from cyclic load-embedment tests, that are not easy to perform. The model uses one set of springs to represent the wood embedment response, and accounts for fastener friction by coupling the frictional response to the wood embedment response. For zero lateral displacement, no force exists in the lateral wood embedment spring, which predicts incorrectly that the fastener is free to withdraw from the wood medium. Some monotonic loading fastener models (Erki 1991, Smith 1983, Nishiyama and Ando 2003) have noted this problem and have therefore modeled the embedment and withdrawal responses using two uncoupled springs to represent the response in both directions. This approach is appropriate for the monotonic case, however, for the cyclic case where the fastener does not always bear on the wood medium, this approach cannot be used.

The difference between wood embedment curves for inserted and driven fasteners has been generally noted for monotonic loading cases (Foschi 1974, Foschi and Bonac 1977, Erki 1991, Smith 1983). The approximate approaches used in deriving embedment curves for driven fasteners for the monotonic case include: the modification of inserted fastener embedment curve (Foschi and Bonac 1977), development of new curves for driven fasteners (Erki 1991), and the modeling of the initial confining pressure as a foundation residual stress (Smith 1983).

The half-hole and full-hole methods stipulated in ASTM 5764-97a (ASTM 1999b) are the current standard methods for measuring the wood embedment response. The half-hole method is preferred (Smart 2002) since bending of the fastener in the full-hole method affects the results obtained. The problem of fastener bending during such load-embedment tests has been noted to be the main source of error in various studies (Rodd *et al.* 2000, Foschi *et al.* 2000b, Smart 2002, Nishiyama and Ando 2003). The half-hole method, however, does not account for the initial confining pressure around the fastener.

The model by Foschi (2000) is similar to Chui *et al.*'s one spring set model, however in Foschi's model, unload/reload occur along a line parallel to the initial stiffness and the slack zone is characterized by a zero force and stiffness condition. As such, the model does not depend on cyclic load-embedment tests as in the case of Chui *et al.* The model has been implemented into a general purpose program module called HYST that is used extensively in the development of 2-D and 3-D wood shear wall and frame analysis programs (e.g., FRAME and LIGHTFRAME3D). The model has been widely validated for various dowel-type connections under various cyclic loading protocols and earthquake ground motions (Wong 1999, Foschi *et al.* 2000a, Schreyer *et al.* 2004), and 2-D and 3-D shear wall buildings with/without openings, under cyclic lateral loading (He *et al.* 2001, Gu and Lam 2004). These have all shown the versatility of the Foschi connector model, and a recent

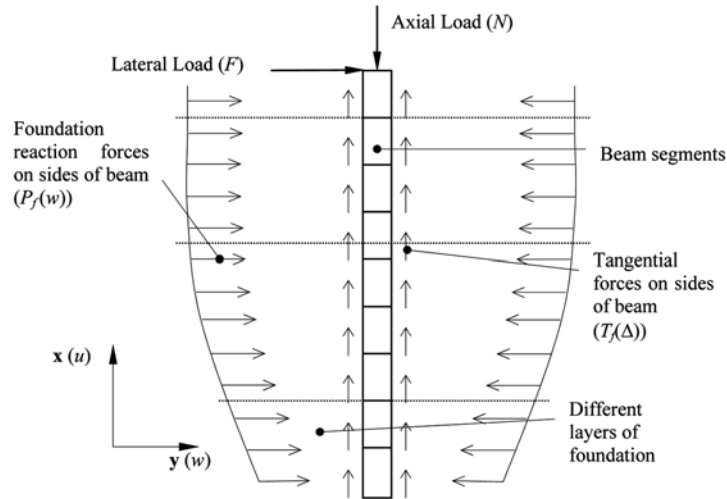


Fig. 1 Schematic of wood-fastener system

state-of-the-art article by Lam *et al.* (2004) has stressed the usefulness of the model in performance-based seismic design. Further information on the various applications of the model can be found online (<http://www.civil.ubc.ca/FRBC>).

1.1 Objectives of study

Since Foschi's connector model has been widely validated but does not account for shaft friction, the objective of this study is to extend the model to account for shaft friction using a consistent physics-based approach. The second part of the study focuses on using the newly developed model to evaluate the effect of friction on two dowel-type connector examples (nail and bolt) that have previously been extensively studied by Foschi.

2. Component modelling

Fig. 1 shows a schematic of a generic beam-foundation system under both axial and lateral loading. This loading is resisted by the extension/compression in the beam element, side frictional forces and lateral foundation pressure.

2.1 Modeling of embedment response

The monotonic load-embedment curve that corresponds to the envelope of the cyclic response represents both the elastic and plastic deformations that occur in the wood medium. The load-embedment curve used to model the medium is the 6-parameter curve by Foschi (2000) shown in Fig. 2 and described by Eq. (1).

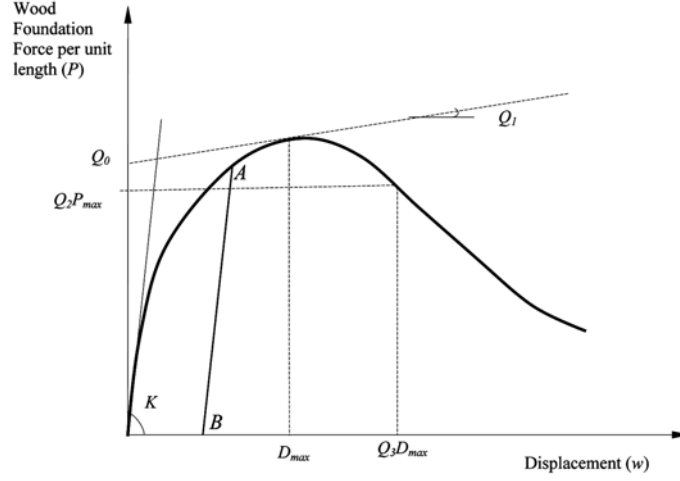


Fig. 2 Schematic of Foschi's wood load-embedment curve

$$P_e = \begin{cases} (Q_0 + Q_1 w)(1.0 - e^{-Kw/Q_0}) & \text{if } w \leq D_{\max} \\ P_{\max} e^{-Q_4(w - D_{\max})^2} & \text{if } w > D_{\max} \end{cases} \quad (1)$$

where $P_{\max} = (Q_0 + Q_1 D_{\max})(1.0 + e^{-KD_{\max}/Q_0})$ and $Q_4 = \ln(Q_2)/[D_{\max}(Q_3 - 1.0)]^2$.

The embedment action is only compressive in nature, and results in the formation of gaps between the beam and the medium, when the load is removed. When an initial confining pressure exists, this must first be overcome before the formation of gaps is possible. The major factors that influence the confining pressure are: the viscoelastic properties of wood; humidity and moisture content; state of wood — green or dry; drying process; type of fastener; and the method of driving.

Because the main difference between driven and inserted fasteners is the initial confining pressure, it is desirable to have a general modeling technique that can be used for both cases. This is against the backdrop that under the same fastener-wood condition for cases where wood splitting is not critical, the embedment curve is mainly a characteristic of the wood medium (Smart 2002).

In this model, we model the embedment curve for both driven and inserted fasteners with the same curve (i.e., embedment curve from half-hole test), but with an existing initial pressure at zero fastener displacement. This is achieved by a lateral leftwards shift of the load-embedment curve as shown in Fig. 3(a). Using this approach, the components of the foundation pressure at a given point along the fastener can be represented by the sum of independent load-embedment responses on the right and left sides of the fastener (Fig. 3b).

Similar to Foschi's approach, loading on each side proceeds along the embedment curve and unloading/reloading also occurs along a line parallel to the initial stiffness (line A-B in Fig. 2). Using this modeling approach, gaps can develop only when the initial confining pressure is exceeded, which is what is observed from experiments (Smith 1983, Erki 1990). Three different types of foundation responses can thus be modeled with this approach, these are: when no initial pressure exists and the fastener bears on at most one side at a given time; when an initial pressure exists and is never overcome; and when an initial pressure exists but is later overcome (Allotey 1999).

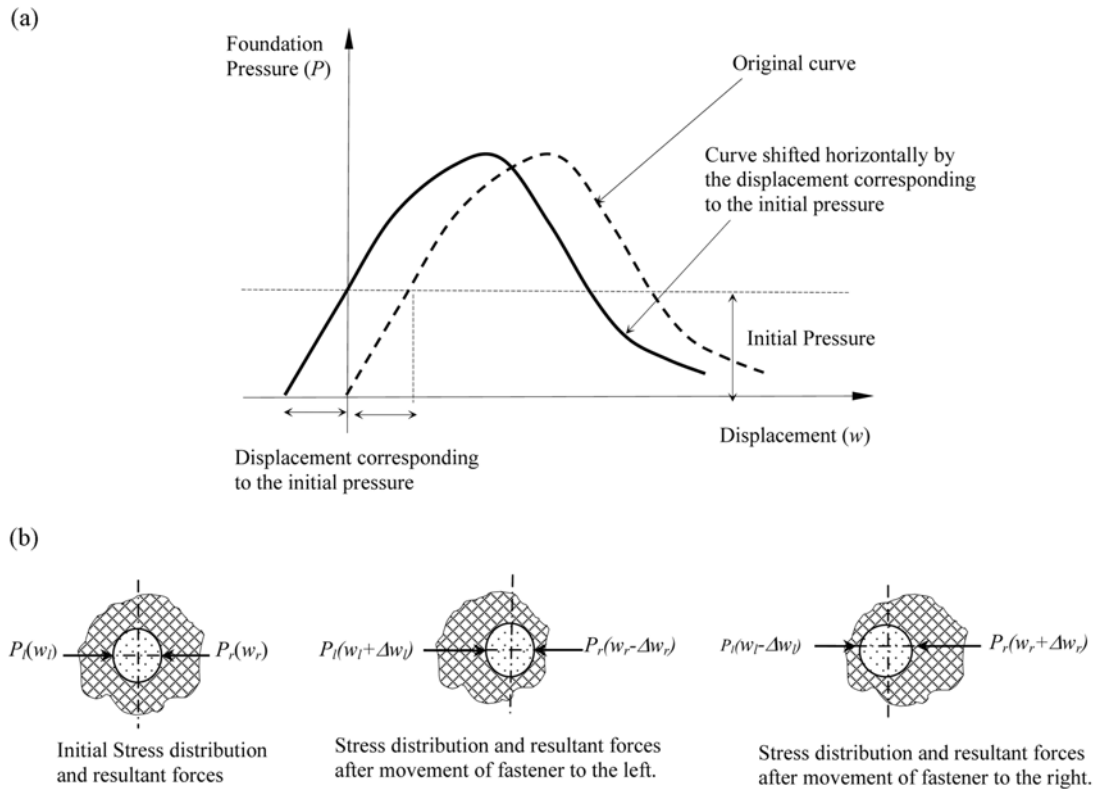


Fig. 3 (a) Shift in wood embedment curve to account for initial confining pressure, (b) Stress distribution and corresponding resultant normal forces on both sides of fastener due to fastener movement in a given direction

2.2 Modeling of tangential response

Withdrawal of driven fasteners under lateral loading has been observed in lateral cyclic shear wall testing by many researchers. The withdrawal response is generally governed by friction. Friction is generally modeled in the field of contact mechanics using a plasticity-type of formulation. Classical Coulomb friction herein referred to as rigid Coulomb friction describes the gross sliding between two effectively rigid bodies, and does not model the deformations occurring on a point-wise basis (Oden and Pires 1983). When the surfaces of two deformable bodies in contact move relative to each other, elastic and inelastic deformations of the junctions between the surfaces occurs until the junction eventually fractures. The interface therefore possesses a finite stiffness against lateral displacement. The two main models used in the literature to model this are elastic Coulomb friction models, and nonlinear friction models, which are characterized by a specified nonlinear function (Oden and Pires 1983).

Typical nail withdrawal tests are performed according to ASTM D1761-88 (ASTM 1999a). It can be observed from these tests that before full slip occurs, the interface can be represented with a finite stiffness as assumed in elastic Coulomb friction theory. An elastic Coulomb friction model is therefore used in this study to model the tangential load-slip response. Fig. 4 shows a schematic of

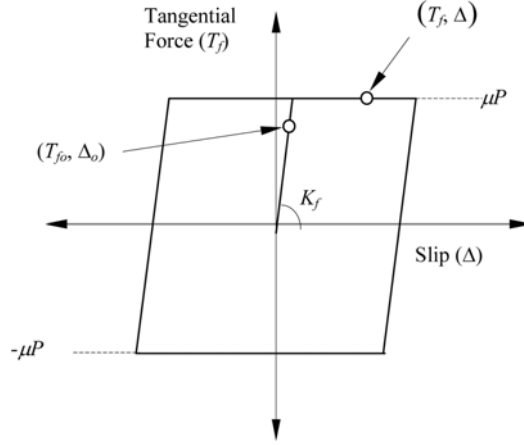


Fig. 4 Schematic of tangential load – slip curve

the model, which is described by Eq. (2), where K_f and μ are the effective tangential stiffness and the coefficient of friction, and T_{f_o} and Δ_o are the tangential force and slip at a prior state.

$$T_f(\Delta) = \begin{cases} 0 & \text{if } P = 0 \\ T_{f_o} + K_f(\Delta - \Delta_o) & \text{if } -\mu P \leq T_f \leq \mu P \\ \mu P & \text{if } T_f > \mu P \\ -\mu P & \text{if } T_f < -\mu P \end{cases} \quad (2)$$

2.3 Modeling of fastener response

A bilinear elastic-perfectly-plastic model, given in Eq. (3) is used to model stress-strain behavior of the fastener. More advanced models that account for strain-hardening could be used, however, since we are mainly interested in assessing the effect of the initial confining pressure and friction, this model is suitable. In the equation, E is the Young's modulus of the fastener, σ_y is the yield stress and $(\sigma_o, \varepsilon_o)$ is the longitudinal stress-strain combination at a prior state.

$$\sigma(\varepsilon) = \begin{cases} \sigma_o + E(\varepsilon - \varepsilon_o) & \text{if } -\sigma_y \leq \sigma \leq \sigma_y \\ \sigma_y & \text{if } \sigma > \sigma_y \\ -\sigma_y & \text{if } \sigma < -\sigma_y \end{cases} \quad (3)$$

3. Derivation of governing equations and FE implementation

Fig. 5 shows a schematic of an elemental portion of the fastener with the various imposed forces. Similar to the model by Foschi (2000), in deriving the governing equations, small displacement theory is assumed and the frame of reference is not updated.

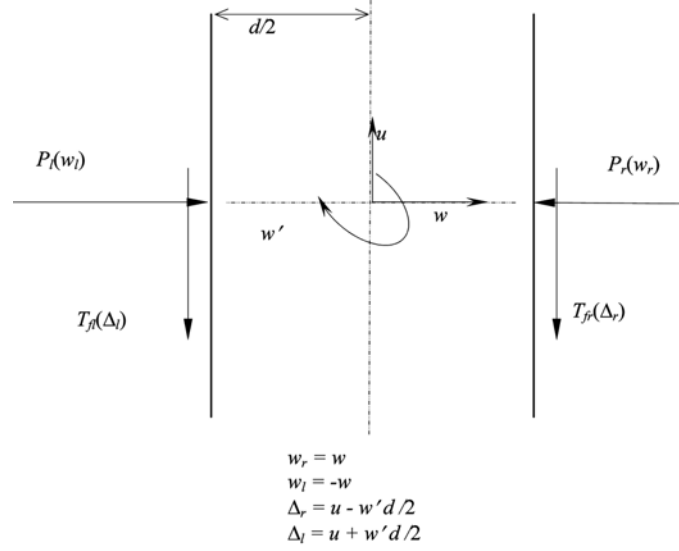


Fig. 5 Free-body diagram of an elemental fastener length

3.1 Kinematics

The fastener is assumed to follow the Euler-Bernoulli hypothesis of cross-sections perpendicular to the centroidal locus before bending, remaining plane and perpendicular to the deformed locus after bending. The only strain of interest is the longitudinal strain. Based on Von Karman's strain-displacement relationship, the longitudinal strain is given by:

$$\varepsilon = \frac{\partial u}{\partial x} - y \frac{\partial^2 w}{\partial x^2} + \frac{1}{2} \left(\frac{\partial w}{\partial x} \right)^2 \quad (4)$$

where u and w are axial displacement and lateral deflection of the fastener. From Eq. (4) moderate strains and P-delta ($P - \delta$) effects are accounted for.

3.2 Equilibrium equations

From the principle of virtual work for a kinematically admissible variation in the displacement ($\delta \mathbf{u}$), the internal and external virtual work are given by:

$$\delta W_{\text{int}} = \int_v \sigma(\varepsilon) \delta \varepsilon dv \quad (5)$$

$$\delta W_{\text{ext}} = - \int_0^L (P_r(w_r) \delta w_r + P_l(w_l) \delta w_l) dx - \int_0^L (T_{fr}(\Delta_r) \delta \Delta_r + T_{fl}(\Delta_l) \delta \Delta_l) dx - N \delta u_{x=L} + F \delta w_{x=L} \quad (6)$$

where v and L are the volume and length of the fastener, respectively. Substituting for w_r , w_l , Δ_r , Δ_l and moving the normal and tangential terms to the internal virtual work side of the equation gives:

$$\int_v \sigma \delta \varepsilon dv + \int_0^L (P_r \delta w - P_l \delta w) dx + \int_0^L \left(T_{fl} \delta \left(u - \frac{d}{2} w' \right) + T_{fr} \delta \left(u + \frac{d}{2} w' \right) \right) dx = -N \delta u_{x=L} + F \delta w_{x=L} \quad (7)$$

From Eq. (7), the tangential forces on left and right sides of the fastener (T_{fr} , T_{fl}) element depend on the normal forces on either side (P_r , P_l). This accounts for coupling between the normal and tangential responses.

3.3 FE implementation and solution procedure

Similar to the approach by Foschi (2000), the fastener displacements $u(x)$ and $w(x)$ are represented, respectively, by cubic and fifth-order polynomials. The vector of degrees of freedom for a fastener element with nodes i and j is thus given by:

$$\mathbf{a}^T = (w_i, w_i', w_i'', u_i, u_i', w_j, w_j', w_j'', u_j, u_j') \quad (8)$$

The finite element approximations to the displacements and their corresponding derivatives are:

$$u(x) = \mathbf{N}^T \mathbf{a}, \quad u'(x) = \mathbf{N}'^T \mathbf{a}, \quad w(x) = \mathbf{M}^T \mathbf{a}, \quad w'(x) = \mathbf{M}'^T \mathbf{a}, \quad w''(x) = \mathbf{M}''^T \mathbf{a} \quad (9)$$

where \mathbf{N} and \mathbf{M} , represent the vector of shape functions.

From Eq. (9) the strain at any point in a fastener element with respect to the nodal degrees of freedom can be expressed as:

$$\varepsilon = (\mathbf{N}'^T - \gamma \mathbf{M}''^T) \mathbf{a} + \frac{1}{2} \mathbf{a}^T \mathbf{M}' \mathbf{M}'^T \mathbf{a} \quad (10)$$

and the fastener internal virtual work given by:

$$\int_v \sigma \delta \varepsilon = \delta \mathbf{a}^T \int_v \sigma [(\mathbf{N}'^T - \gamma \mathbf{M}''^T) + \mathbf{M}' \mathbf{M}'^T] \mathbf{a} dv \quad (11)$$

The work done by the normal and tangential pressures are:

$$\int_0^L (P_r \delta w - P_l \delta w) dx = \delta \mathbf{a}^T \int_0^L (P_r - P_l) \mathbf{M} dx \quad (12)$$

$$\int_0^L \left(T_{fr} \delta \left(u - \frac{d}{2} w' \right) + T_{fl} \delta \left(u + \frac{d}{2} w' \right) \right) dx = \delta \mathbf{a}^T \int_0^L \left[(T_{fl} + T_{fr}) \mathbf{N} + \frac{d}{2} (T_{fl} - T_{fr}) \mathbf{M}' \right] dx \quad (13)$$

Also, that done by the external axial and lateral loads is:

$$-N \delta u_{x=L} + F \delta w_{x=L} = \delta \mathbf{a}^T (-N \mathbf{N}_{x=L} + F \mathbf{M}_{x=L}) \quad (14)$$

Following standard finite element techniques, the Newton-Raphson (NR) procedure is used to solve for the global solution vector. The solution procedure is augmented with a line search technique to enhance the solution procedure. Both displacement and force convergence criteria are used to check

for convergence. Based on the NR implementation, the expression for the out-of-balance force vector is given by:

$$\Psi = \Psi_l + \Psi_\sigma + \Psi_e + \Psi_f + NN_{x=L} - FM_{x=L} \quad (15)$$

where, Ψ_l , Ψ_σ , Ψ_e , and Ψ_f represent the linear, geometric, normal and tangential parts of the force vector. Similarly, the expression for the consistent tangent stiffness matrix is:

$$\mathbf{K}_t = \mathbf{K}_l + \mathbf{K}_\sigma + \mathbf{K}_e + \mathbf{K}_f \quad (16)$$

where, again \mathbf{K}_l , \mathbf{K}_σ , \mathbf{K}_e and \mathbf{K}_f represent the linear, geometric, normal and tangential parts of the stiffness matrix.

4. Parametric study

From the developed formulation a new version of HYST was developed for modeling the cyclic response of laterally loaded timber fasteners. Two example problems studied by Foschi (2000) were

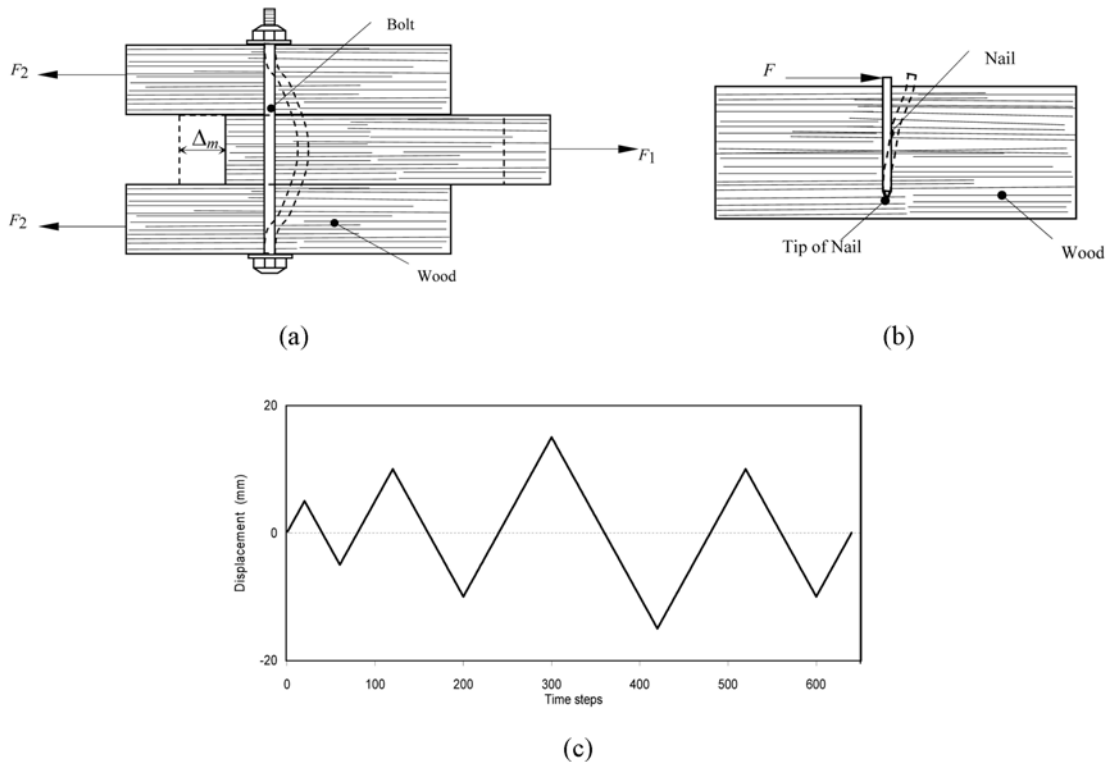


Fig. 6 Schematic of (a) three wood layer bolted connection, (b) nail fastener in wood medium, (c) imposed reversed cyclic loading history

chosen to observe the response of the different model parameters on the cyclic response. These examples were chosen since all the necessary input data and computed hysteresis loops were available (Foschi 2000), making the verification of the new model straightforward. The results obtained from the parameter study, although specific to this study, are helpful in understanding the effect of the various parameters on the fastener embedment-withdrawal response under cyclic loading. This is especially so since based on the author's knowledge the literature does not currently contain such information. The problems studied were a single driven fastener (nail, dowel) in wood, and a single bolt connecting three wood layers (Figs. 6a and 6b). The input loading history used by Foschi was a varying reversed cyclic loading history as shown in Fig. 6(c).

The comparison of the results for the case of no friction and initial confining pressure with those obtained by Foschi (2000) showed an exact match. This can be identified from Figs. 7 and 8, as the hysteresis loops for low values of the initial confining pressure and friction. This validated the changes made to the original model, and these two example problems were then used for the parametric study.

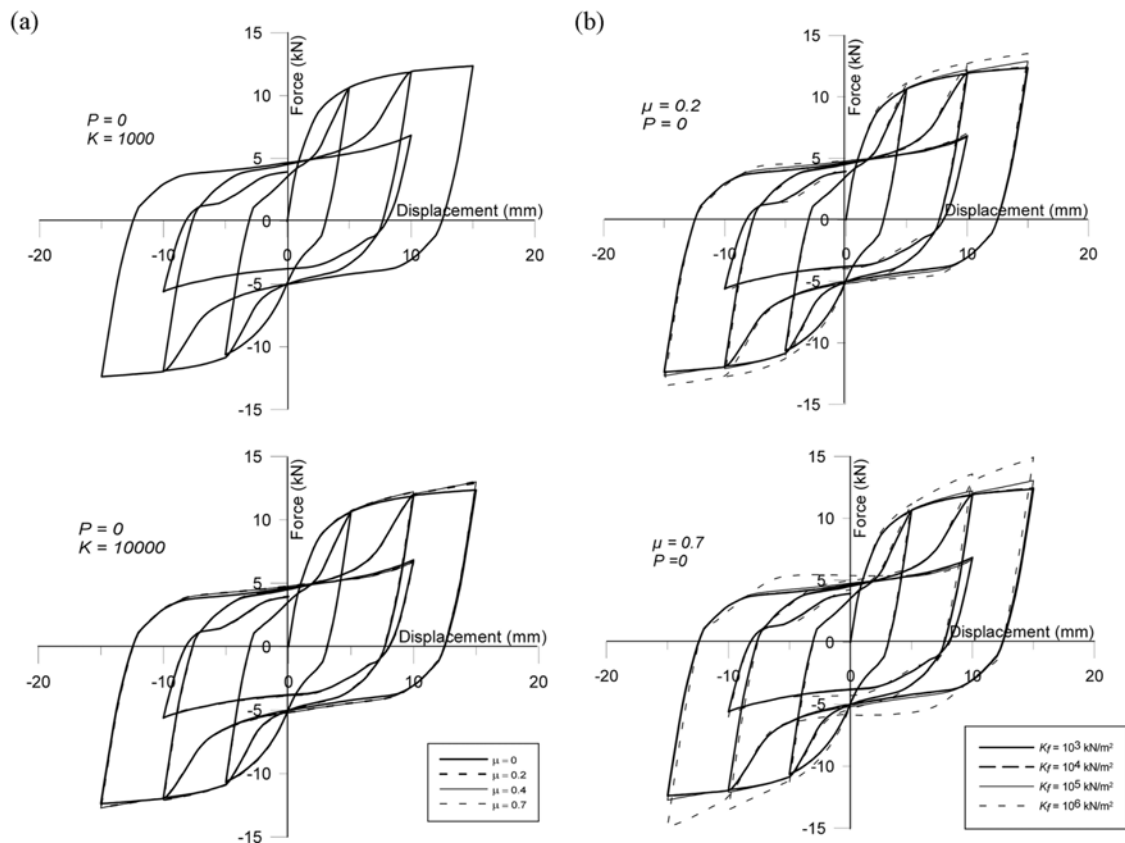


Fig. 7 Effect of (a) coefficient of friction and (b) effective elastic tangential stiffness on cyclic hysteretic response of bolted connection

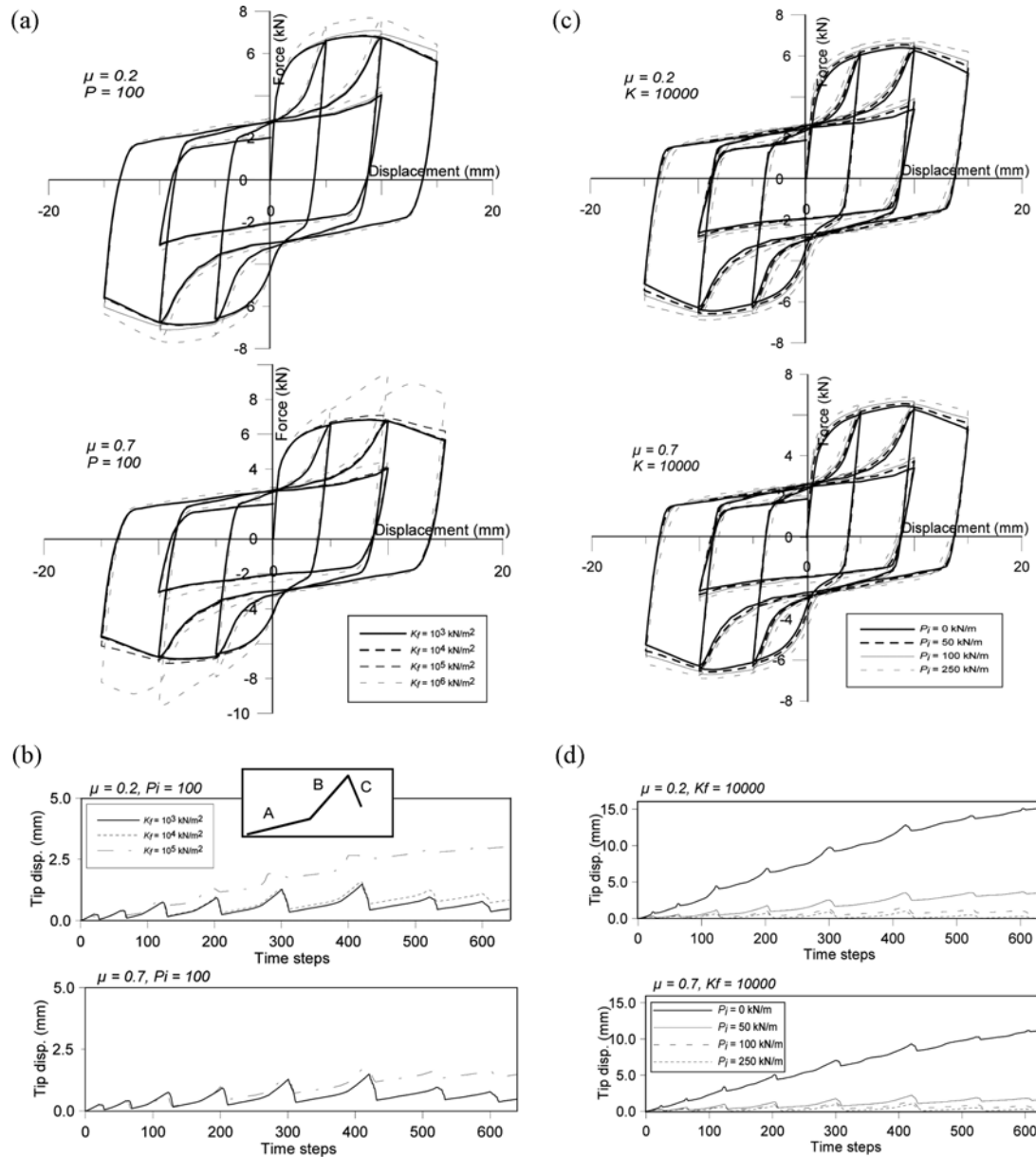


Fig. 8 Effect of effective elastic tangential stiffness on (a) cyclic hysteresis response; and (b) tip displacement and effect of initial confining pressure on (c) cyclic hysteresis response; and (d) tip displacement history of single nail in wood medium

4.1 Parameter estimation

4.1.1 Coefficient of friction

The value of the coefficient of friction between the fastener and wood medium can be determined using ASTM G115-04 (ASTM 2004). The Wood Handbook (UFPA 1974) gives values of μ for

unpolished steel on dry and green wood as 0.7 and 0.4; and when in the presence of lignum vitae as 0.2 and 0.34, respectively. From the technical specifications of a number of wood product companies using timber with specific gravities ranging between 0.5-0.75, the value of μ quoted varied between 0.4-0.6 for dry wood, and 0.55-0.85 for wet wood. From the literature, the values of μ used by various researchers show quite a difference. For example, Wilkinson and Rowlands (1981) used a value of 0.7 in their 2-D finite element analysis of a bolted joint, while based on Erki's experimental work, Chui *et al.* (1998) used a value of 0.1. Guan and Rodd (2000) also used a value of μ equal to 0.75 in their finite element analysis of reinforced timber joints. A range of μ between 0-0.8 was thus used in this study.

4.1.2 Effective tangential stiffness

This parameter can be approximately estimated from nail withdrawal tests (e.g., Wolf 2000, Nishiyama and Ando 2003). In estimating K_f , it was assumed that the fastener was axially inextensible under withdrawal loading, and that the frictional force per unit length is the same over the entire length of the fastener. From these assumptions, the expression for the resultant tangential force at a point, on one side of the beam is, $T_f = N/(2L)$. Correspondingly, the effective tangential stiffness is given by:

$$K_f = \frac{N}{2L\delta_w} \quad (17)$$

where δ_w is the tangential displacement. From various withdrawal load tests (Table 1) K_f was chosen to vary between 10^3 - 10^6 kN/m² (a three order of magnitude difference).

4.1.3 Initial confining pressure

Since no measurements of the initial confining pressure are available in the literature, an approximate estimate of it was computed. Similar to the assumptions used in estimating K_f , the confining pressure is assumed to be constant along the length of the assumed axially inextensible fastener. Based on this, the confining pressure can be computed as:

Table 1 Estimated initial confining pressures and effective tangential stiffnesses

Estimated elastic effective stiffness (kN/m ²)		
UFPA (1974)	8000-23000	
Rammer <i>et al.</i> (2001)	2000-30,000	
Wolf (2000)	1500-5000	
Estimated initial confining pressure (kN/m)		
	$\mu = 0.1$	$\mu = 0.7$
UFPA (1974)	70	9.5
AFPA (1993)	8-130	1-20
Chui and Craft (2002)	55-90	8-14
Rammer <i>et al.</i> (2001)	10-50	2-8
Sutt <i>et al.</i> (2000)	20-35	2-5
Wolf (2000)	50	7

$$P_i = \frac{N}{\mu\pi L} \quad (\text{force per unit length}) \quad (18)$$

Table 1 shows values of the confining pressure estimated based on Eq. (18) and withdrawal load estimates from various design handbooks and fastener withdrawal load tests. Based on this, an initial confining pressure range of 0-250 kN/m was chosen. This range was estimated using expected estimates of the coefficient of friction. From the results, a pressure of 250 kN/m is unlikely, however, this was chosen to represent an upper bound.

4.1.4 Comments

From the above, to obtain all the necessary parameters of the model, three different tests have to be performed (wood embedment test — ASTM 1999b; fastener withdrawal test — ASTM 1999a, dynamic friction test — ASTM 2004). However, as noted by Nishiyama and Ando (2003) these are all standard tests that are routinely performed in practice. From fastener withdrawal and dynamic friction tests, the initial confining pressure which is typically not a parameter evaluated from such tests can be accurately evaluated by way of Eq. (18). This result is of significant importance since it shows that the model can be fully defined with currently available test procedures.

4.2 Single bolt connection

In this problem it is assumed that there is a pre-drilled hole of similar size to the bolt, hence, the bolt does not experience any initial confining pressure, and the only variables of interest are μ , and K_f . Fig. 6(a) shows the bolt clamped at the ends with a lateral displacement (Δ_m) applied to the middle layer. The diameter of the bolt is 9.52 mm and the thickness of each piece of wood is 50 mm. The Young's modulus and yield stress of the bolt are 200 GPa and 250 MPa, respectively. The 6 parameters of the Foschi's load-embedment curve for this wood specimen with a specific gravity of 0.67 are: $Q_0 = 500$ kN/m; $Q_1 = 1.50$ MN/m²; $Q_2 = 0.5$; $Q_3 = 1.5$; $D_{\max} = 7.5$ mm and $K = 400$ MN/m². Due to symmetry, only half of the bolt was discretized using a total of 6 elements; 2 in the central layer and 4 in the outside layer.

The simulated hysteretic response of the three-wood-layer bolted connection for different combinations of μ , and K_f is shown in Fig. 7. Fig 7(a) shows the influence of the coefficient of friction on the hysteretic response of the system for two values of the effective tangential stiffness 10^4 kN/m² and 10^5 kN/m². Fig. 7(b) also shows the influence of K_f on the hysteretic response for a coefficient of friction of 0.2 and 0.7. From both figures, the basic shapes of the hysteresis loops do not change with a variation in any of the variables. It can be seen that for lower values of K_f , which represents the expected stiffness range as shown in Table 1, friction does not significantly affect the computed response. For higher values of K_f , it is observed that there is an increase in the ultimate load, which gets more significant for higher values of the coefficient of friction.

4.3 Single nail connection

In this problem it was assumed that the nail was driven and therefore experiences an initial confining pressure. Under lateral loading, the tip of the nail (bottom of the nail) can be displaced vertically, i.e., withdraw from the wood. Since the model is based on small displacement theory, only relatively moderate axial displacements can be accurately predicted. The lateral cyclic

displacement history is applied to the top of the nail as shown in Fig. 6(b). The variables of interest in this case are μ , K_f and P_i . The length of the nail is 63.5 mm with a diameter of 9.52 mm. The specifications for all other variables are the same as in the bolted connection example, except that the nail is discretized into 5 elements. The cyclic hysteretic response and corresponding tip displacements are shown in Fig. 8.

4.3.1 Hysteretic response

From Fig. 8(c) we observe that for $K_f = 10^4$ kN/m² the initial confining pressure does not significantly influence the hysteretic response. The initial lateral stiffness of the system however increases with increasing initial confining pressure. From Table 1 most of the estimated confining pressures are below 100 kN/m, and the increase in energy dissipated by the system (area enclosed by curves) compared to the case of no initial confining pressure is less than 5%. This is in contrast to Fig. 8(a) where increasing K_f results in an increase in the corresponding ultimate load, similar to what was observed in the bolt example. The concept of an increase in the ultimate load as a result of friction was also noted by Rodd (1988) in his experimental work on the effect of normal and frictional forces between wood and a circular dowel. This is due to the activation of larger frictional forces for larger K_f values under large displacements (Smart 2002). Smaller values of K_f which fall within the practical stiffness range shown in Table 1 however do not show any significant increase.

4.3.2 Withdrawal response

From Figs. 8(b) and 8(d), it is observed that for all the cases studied there is a cumulative withdrawal of the nail under the imposed loading history. Comparing the input displacement history, computed hysteresis curves and the tip displacement history, it is observed that the localized decrease in tip displacement (section C) corresponds to the points where unloading of the fastener occurs. From Eq. (19), the tip displacement is a summation of elastic and inelastic fastener strain displacements, and slip between the fastener and wood medium.

$$u_{tip} = \sum_L \varepsilon_{elastic} + \sum_L \varepsilon_{inelastic} + \sum_L \Delta_{slip} \quad (19)$$

Of the three, only the elastic strain displacements are recoverable, and from the observation made above, it can be confirmed that localized decreases in displacement are the elastic parts of the tip displacement history. Fig. 7(b) shows that this phenomenon decreases with increase in K_f . This can be explained by the fact that as K_f increases, slippage occurs at smaller displacements, resulting in increased slippage as opposed to that of fastener straining. In such cases the coefficient of friction has more effect on the response as observed from the hysteretic response. Oden and Pires (1984) also noted a similar occurrence in their study of the influence of a wide range of K_f values on the elastic contact stress distribution between a deformable half-space and a rigid foundation.

Section B is linked to the rising portions of the hysteresis curves and represents the stage where the fastener begins to bear once again on the wood medium. At this stage, the straining of the fastener increases and most of the inelastic strain displacement of the fastener occurs. Section A is also linked to the stage where the fastener moves in the slack region, and is the stage where most of the amount of fastener slip occurs. Sample plots of the shape of the nail and the corresponding holes existing at given displacement steps can be found in Allotey (1999).

In Fig. 8(d), for $P_i = 0.0$ kN/m, maximum displacements obtained were around 15 mm

representing about 20% of the nail length. However, because the model is based on small displacement theory this cannot be trusted. More reasonable results were obtained for other confining pressures, and it can be noted that the initial confining pressure considerably affects the maximum tip displacement. This decrease can be attributed to the fact that confining pressure restrains slippage and causes more straining of the fastener. This clearly shows that the presence of an initial confining pressure substantially reduces the amount of nail withdrawal. Under such conditions, the ratio of the contribution of inelastic strain displacement to the tip permanent displacement increases. Figs. 7 and 8 also show that an increase in the coefficient of friction results in a decrease in tip displacement, which is common-knowledge.

5. Conclusions

This paper focused on the extension of Foschi's connector model to account for shaft friction. A consistent methodology was developed for including the effect of shaft friction and initial confining pressure. The method was based on using two springs to model the load-embedment behaviour, with each spring shifted to the left to account for an initial confining pressure at zero fastener displacement. Shaft friction was also modeled using an elastic Coulomb friction model. A significant advantage of this approach when compared to others is that it correctly models the coupling between the lateral and withdrawal responses of the fastener. Another attractive feature of the model is that parameters needed to fully define it can be directly obtained from standard routine tests.

The results obtained from a parametric study of the influence of the different model parameters on the cyclic response showed that:

- i. The initial confining pressure does not have a significant effect on the hysteretic response, but plays a very important role in reducing the amount of nail withdrawal.
- ii. For practical ranges of the coefficient of friction and effective tangential stiffness, friction does not have a significant effect on the hysteretic response, but considerably affects the amount of nail withdrawal.

Even though the results obtained are specific to this study, they give a general idea of the influence of the different model parameters on the cyclic response of such fastener connections.

These results point to the fact that cyclic fastener models that do not account for friction (e.g., Foschi 2000) are suitable for the analysis of the lateral cyclic response of timber joints, provided the amount of fastener withdrawal is not significant. This underlies the reason why Foschi's connector model has been known to perform satisfactorily when used in modeling different types of connections.

Acknowledgements

Financial support for this study was provided by a research grant to the senior author (reference number — PA97474-1RE) from Forest Renewal British Columbia (FRBC) for the project, Reliability and Design of Innovative Wood Structures under Earthquake and Extreme Wind conditions.

References

- Allotey, N.K. (1999), "A model for the response of single timber fasteners and piles under cyclic and dynamic loading", M.A.Sc. Thesis, University of British Columbia, Vancouver, B.C.
- American Forest and Paper Association (AFPA, 1993), *National Design Specification for Wood Construction*, American Forest and Paper Association, Washington, D.C.
- American Society for Testing and Materials (ASTM, 1999a), "D1761-88 — Standard test methods for mechanical fasteners in wood", *1999 Annual Book of ASTM Standards*, Vol. 04.10, ASTM, West Conshohocken, Pennsylvania.
- American Society for Testing and Materials (ASTM, 1999b), "D5764-97a — Standard test method for evaluating dowel-bearing strength of wood and wood-based products", *1999 Annual Book of ASTM Standards*, Vol. 04.10, ASTM, West Conshohocken, Pennsylvania.
- American Society for Testing and Materials (2004), "G115-04 — Standard guide for measuring and reporting friction coefficients", *2004 Annual Book of ASTM Standards*, Vol. 04.03, ASTM, West Conshohocken, Pennsylvania.
- Chui, Y.H., Ni, C. and Jiang, L. (1998), "Finite element model for nailed wood joints under reversed cyclic load", *J. Struct. Engrg.*, ASCE, **124**(1), 96-103.
- Chui, Y.H. and Craft, S. (2002), "Fastener head pull-through of plywood and oriented strand board", *Can. J. Civ. Engrg.*, **29**, 384-388.
- Durham, J., Lam, F. and Prion, H.G.L. (2001), "Seismic resistance of wood shear walls with large OSB panels", *J. Struct. Engrg.*, ASCE, **127**(12), 1460-1466.
- Erki, M.A. (1991), "Modeling the load-slip behavior of timber joints with mechanical fasteners", *Can. J. Civ. Engrg.*, **18**, 607-616.
- Foliente, G. (1995), "Hysteresis modeling of wood joints and structural systems", *J. Struct. Engrg.*, ASCE, **121**(6), 1013-1022.
- Folz, B. and Filiatrault, A. (2001), "Cyclic analysis of wood shear walls", *J. Struct. Engrg.*, ASCE, **127**(4), 433-441.
- Foschi, R.O. (1974), "Load-slip characteristics of nails", *Wood Sci.*, **7**, 69-74.
- Foschi, R.O. and Bonac, T. (1977), "Load-slip characteristics for connections with common nails", *Wood Sci.*, **9**, 118-123.
- Foschi, R.O. (2000), "Modeling the hysteretic response of mechanical connections for wood structures", *Proc. 6th World Conf. Timber Engrg.*, University of British Columbia, Vancouver, B.C.
- Foschi, R.O., Yao, F. and Rogerson, D. (2000a), "Determining embedment response parameters from connector tests", *Proc. 6th World Conf. Timber Engrg.*, University of British Columbia, Vancouver, B.C.
- Foschi, R.O., Ventura, C., Lam, F. and Prion, H.G.L. (2000b), "Reliability and design of innovative wood structures under earthquake and extreme wind conditions", FRBC Research Project Report, Department of Civil Engineering, University of British Columbia, Vancouver, B.C., online (www.civil.ubc.ca/FRBC).
- Guan, Z.W. and Rodd, P.D. (2000), "Three-dimensional finite element model for locally reinforced timber joints made with hollow dowel fasteners", *Can. J. Civ. Engrg.*, **27**, 785-797.
- Gu, J. and Lam, F. (2004), "Simplified mechanics-based wood frame shear wall model", *13th World Conf. Earthquake Engineering*, Vancouver, B.C., Paper No. 3109.
- He, M., Magnusson, H., Lam, F. and Prion, H.G.L. (1999), "Cyclic performance of perforated wood shear walls with oversized OSB panels", *J. Struct. Engrg.*, ASCE, **125**(1), 10-18.
- He, M., Lam, F. and Foschi, R.O. (2001), "Modeling three-dimensional timber light-frame buildings", *J. Struct. Engrg.*, ASCE, **127**(8), 901-913.
- Lam, F., Filiatrault, A., Kawai, N., Nakajima, S. and Yamaguchi, N. (2004), "Performance of timber buildings under seismic load: Part 2: Modeling", *Prog. Struct. Engrg. Mater.*, **6**, 79-83.
- Moses, D.M. (2000), "Constitutive and analytical modeling of structural composite lumber with applications in bolted connections", Ph.D. Thesis, University of British Columbia, Vancouver, B.C.
- Nishiyama, N. and Ando, N. (2003), "Analysis of load-slip characteristics of nailed wood joints: Application of a two-dimensional geometric nonlinear analysis", *J. Wood Sci.*, Japan Wood Research Society, **49**, 505-512.
- Oden, J.T. and Pires, E.B. (1984), "Algorithms and numerical results for finite element approximations of contact

- problems with non-classical friction laws”, *Comp. Struct.*, **19**, 137-147.
- Oden, J.T. and Pires, E.B. (1983), “Nonlocal and nonlinear friction laws and variational principles for contact problems in elasticity”, *J. App. Mech.*, **16**, 67-75.
- Rammer, D.R., Winistofer, S.G. and Bender, D.A. (2001), “Withdrawal strength of threaded nails”, *J. Struct. Engrg.*, ASCE, **127**(4), 442-449.
- Rodd, P.D. (1988), “Timber joints made with improved circular dowel fasteners”, *Proc. 1st Int. Conf. Timber Engrg.*, Seattle, WA., **1**, 26-37.
- Rodd, P.D., Guan, Z.W. and Pope, D.J. (2000), “Measurement and rationalization of fastener embedment data”, *Proc. 6th World Conf. Timber Engrg.*, University of British Columbia, Vancouver, B.C.
- Schreyer, A.C., Lam, F. and Prion, H.G.L. (2004), “Comparison of slender dowel-type fasteners for slotted in steel plate connections under monotonic and cyclic loading”, *Proc. 7th World Conf. Timber Engrg.*, Finish Association of Civil Engineers, Helsinki, Finland.
- Smart, J.V. (2002), “Capacity resistance and performance of single-shear bolted and nailed connections: an experimental investigation”, M.Sc. Thesis, Virginia Polytechnic Institute and State University, Blacksburg, Virginia.
- Smith, I. (1983), “Short-term load deformation relationships for timber joints with dowel-type connectors”, Ph.D. Thesis, Polytechnic of the South Bank, CNAA.
- Sutt, E., Reinhold, T. and Rosowsky, D. (2000), “The effect of in-situ conditions on withdrawal capacities”, *Proc. 6th World Conf. Timber Engrg.*, University of British Columbia, Vancouver, B.C.
- U.S. Forest Products Laboratory (UFPA 1974), *Wood Handbook: Wood as an Engineering Material*, USDA Agricultural Handbook, **72**.
- Wilkinson, T.L. and Rowlands, R.E. (1981), “Analysis of mechanical joints in wood”, *Exp. Mech.*, **21**, 408-441.
- Wolf, T. (2000), “Determination of transverse bending stiffness of nail-laminated timber elements”, *Proc. 6th World Conf. Timber Engrg.*, University of British Columbia, Vancouver, B.C.
- Wong, E. (1999), “Verification of an analytical hysteresis model for dowel-type timber connections using shake table tests”, M.A.Sc. Thesis, University of British Columbia, Vancouver, B.C.

Notation

\mathbf{a}	: Vector of degrees of freedom
d	: Diameter of fastener
D_{\max}	: Displacement corresponding to maximum embedment pressure in Foschi’s embedment curve
E	: Young’s Modulus of Elasticity
F	: Lateral load
i, j	: Nodes of beam element
I	: Moment of inertia about y - y axis
K	: Initial stiffness of Foschi’s wood embedment curve
K_f	: Effective tangential stiffness
\mathbf{K}_i	: Global stiffness matrices
$\mathbf{K}_b, \mathbf{K}_\sigma$: Linear and geometric stiffness matrices
$\mathbf{K}_e, \mathbf{K}_f$: Foundation embedment and frictional stiffness matrices
L	: Length of fastener
u, w	: Axial and lateral displacement of cross-sectional centroid
N	: Axial load
P_e	: Embedment pressure
P_i	: Initial confining pressure
P_l, P_r	: Foundation pressure on the left and right sides of fastener
Q_0, Q_1, Q_2, Q_3, Q_4	: Constants of Foschi’s embedment curve
T_f	: Tangential frictional force per unit length of fastener
T_{fr}, T_{fl}	: Frictional force on the right and left sides of fastener

\mathbf{u}	: Displacement vector
v	: Volume of fastener
w_l, w_r	: Lateral displacement of left and right sides of fastener
x	: Direction along the fastener
y	: Direction perpendicular to fastener
Δ, Δ_0	: Current and previous tangential displacements along interface
Δ_m	: Imposed displacement of middle layer in three layer bolted connection
Δ_r, Δ_l	: Tangential displacement on the right and left sides of fastener
$\varepsilon, \varepsilon_0$: Current and previous strains at a given point in fastener
μ	: Coefficient of friction
σ, σ_0	: Current and previous stresses at a given point in fastener
Ψ	: Global out-of-balance force vectors
Ψ_e, Ψ_f	: Foundation embedment and frictional force vectors
Ψ_b, Ψ_σ	: Linear and nonlinear internal force vectors